



UNIVERSITÀ
DEGLI STUDI
FIRENZE

FLORE

Repository istituzionale dell'Università degli Studi di Firenze

SIRT1 modulates MAPK pathways in ischemic-reperfused cardiomyocytes

Questa è la Versione finale referata (Post print/Accepted manuscript) della seguente pubblicazione:

Original Citation:

SIRT1 modulates MAPK pathways in ischemic-reperfused cardiomyocytes / M. Becatti ; N. Taddei; C. Cecchi; N. Nassi; P.A. Nassi; C. Fiorillo. - In: CELLULAR AND MOLECULAR LIFE SCIENCES. - ISSN 1420-9071. - STAMPA. - 69:(2012), pp. 2245-2260. [10.1007/s00018-012-0925-5]

Availability:

This version is available at: 2158/605600 since: 2019-07-25T21:54:32Z

Published version:

DOI: 10.1007/s00018-012-0925-5

Terms of use:

Open Access

La pubblicazione è resa disponibile sotto le norme e i termini della licenza di deposito, secondo quanto stabilito dalla Policy per l'accesso aperto dell'Università degli Studi di Firenze (<https://www.sba.unifi.it/upload/policy-oa-2016-1.pdf>)

Publisher copyright claim:

(Article begins on next page)

SIRT1 modulates MAPK pathways in ischemic–reperfused cardiomyocytes

Matteo Becatti · Niccolò Taddei · Cristina Cecchi ·
Niccolò Nassi · Paolo Antonio Nassi · Claudia Fiorillo

Received: 1 July 2011 / Revised: 21 December 2011 / Accepted: 19 January 2012
© Springer Basel AG 2012

Abstract SIRT1, an ubiquitous NAD(+)-dependent deacetylase that plays a role in biological processes such as longevity and stress response, is significantly activated in response to reactive oxygen species (ROS) production. Resveratrol (Resv), an important activator of SIRT1, has been shown to exert major health benefits in diseases associated with oxidative stress. In ischemia–reperfusion (IR) injury, a major role has been attributed to the mitogen-activated protein kinase (MAPK) pathway, which is upregulated in response to a variety of stress stimuli, including oxidative stress. In neonatal rat ventricular cardiomyocytes subjected to simulated IR, the effect of Resv-induced SIRT1 activation and the relationships with the MAPK pathway were investigated. Resv-induced SIRT1 overexpression protected cardiomyocytes from oxidative injury, mitochondrial dysfunction, and cell death induced by IR. For the first time, we demonstrate that SIRT1 overexpression positively affects the MAPK pathway—via Akt/ASK1 signaling—by reducing p38 and JNK phosphorylation and increasing ERK phosphorylation. These results reveal a new protective mechanism elicited by Resv-induced SIRT1 activation in IR tissues and suggest novel potential therapeutic targets to manage IR-induced cardiac dysfunction.

Keywords SIRT1 · Ischemia–reperfusion · Oxidative stress · MAPKs

Abbreviations

ASK1	Apoptosis signal-regulating kinase 1
Bcl-xl	B cell lymphoma-extra large
Bcl-2	B cell lymphoma-2
BODIPY	Boron-dipyrromethene
Calcein-AM	Calcein acetoxymethyl ester
DEVD	Asp Glu Val Asp
DMEM	Dulbecco's modified Eagle's medium
DMSO	Dimethyl sulfoxide
EDTA	Ethylenediaminetetraacetic acid
EIA	Enzyme immunoassay
ELISA	Enzyme-linked immunosorbent assay
ERK	Extracellular signal-regulated kinase
FACS	Fluorescence-activated cell sorting
FAM	Fluorescein acetoxymethyl ester
FLICA	Fluorochrome Inhibitor of caspases
FMK	Fluoromethyl ketone
FOXO1	Forkhead box O1
H ₂ DCFDA	2', 7'-Dichlorofluorescein diacetate
JNK	Jun N-terminal kinase
LDH	Lactate dehydrogenase
MAPK	Mitogen-activated protein kinase
MnSOD	Manganese superoxide dismutase
mPTP	Mitochondrial permeability transition pore
PAGE	Polyacrylamide gel electrophoresis
PBS	Buffered saline solution
PMSF	Phenylmethanesulphonyl fluoride
PVDF	Polyvinylidene fluoride
ROS	Reactive oxygen species
Resv	Resveratrol
SD	Standard deviation
SDS	Sodium dodecyl sulphate
SIRT1	Sirtuin (Silent information regulator 2) 1
TAC	Total antioxidant capacity

M. Becatti · N. Taddei · C. Cecchi · N. Nassi ·
P. A. Nassi · C. Fiorillo (✉)
Department of Biochemical Sciences, University of Florence,
Viale GB Morgagni 50, 50134 Florence, Italy
e-mail: claudia.fiorillo@unifi.it

TMRM	Tetramethylrhodamine, methyl ester, perchlorate
Trx1	Thioredoxin-1
UV	Ultraviolet
$\Delta\psi$	Mitochondrial membrane potential

Introduction

In heart, ischemia–reperfusion (IR) has been found to be a major cause of myocyte necrosis and apoptosis. Such processes appear to be the prevalent mode of cell death during the ischemic and the reperfusion phases, respectively. It is widely accepted that the oxidative stress, due to an excessive production of reactive oxygen species (ROS), is a prominent factor in triggering the events that ultimately result in cardiomyocyte death [1, 2]. The intracellular signaling pathways that lead to this effect, however, are relatively poorly understood. A mechanism for cardiomyocyte death during IR has been related to the stress responsive members of the mitogen-activated protein kinase (MAPK) family. A variety of stress stimuli, including oxidative stress, induces functional changes of these kinases, similar to those found associated with apoptosis [3]. A recent finding suggests that cardiac SIRT1, a mammalian ortholog of Silent information regulator 2 (Sir2) family, is significantly upregulated in response to oxidative stress [4]. The members of the Sir2 family, a group of highly conserved proteins showing NAD-dependent histone deacetylase activity, have been indicated as modulators of the life-span in many living species. Some reports suggested that mammalian sirtuins may play a role in DNA repair [5]. An early finding that pointed to a role for Sir2 as a life-span regulator in yeast was later confirmed for SIRT1 [6]. However, increasing evidence suggests that, in mammals, sirtuins may affect the aging process by regulating several processes, such as glucose homeostasis, insulin secretion, fat metabolism, and resistance to stress [7, 8]. SIRT1 was initially thought to be localized exclusively in the cell nucleus; however, recent evidence suggests that the protein shuttles between the nucleus and the cytosol, making it possible to play functions in the cytosolic milieu [9]. SIRT1 targets multiple proteins involved in apoptosis, including p53, p73, E2F, HIC1, and Ku70, and modulates cell survival by regulating the Forkhead family of transcription factors (FOXOs). Acting via FOXO4, SIRT1 also suppresses caspase-3 and caspase-7 in transformed cells, but not in normal cells [10]. Interestingly, caspase-9 and Bcl-xL regulate SIRT1 cleavage during apoptosis, causing it to relocate from the nucleus to the cytosol [11]. A number of recent reports have sought to elucidate the direct effects of SIRT1 in mammalian

tissues. Moderate expression levels of SIRT1 have been shown to slow coronary aging and promote resistance to oxidative stress and apoptosis, suggesting that SIRT1 protects the heart from in vivo stress [4]. In any case, the data currently available in the literature indicating a variety of effects on cellular metabolism and gene expression suggest sirtuins play a role in cardioprotection, as over-expression of SIRT1 protects cardiomyocytes from serum deprivation-induced cell death and promote an increase in cell size [12]. In contrast, sirtuin inhibition triggered cell death in isolated neonatal rat cardiomyocytes [13].

Trans-resveratrol (*trans*-3,4',5-trihydroxystilbene, Resv), a polyphenol of red wine, is one of the substances proposed to be responsible for the prevention of cardiovascular disease, especially in coronary artery disease. Resv reportedly protects the heart from ischemic-reperfusion injury [14]. With regard to cardiomyoblasts, it has been suggested that Resv has direct beneficial effects against ischemia/hypoxia of cardiomyocytes, protecting these cells from apoptosis through the involvement of SIRT1 [15].

The present study aims to assess whether SIRT1 has an effective role in protecting cardiac cells from IR injury and to explore the involvement of this protein in the modulation of typical redox-sensitive MAPKs such as JNK (c-Jun NH₂ terminal kinase), ERK (extracellular signal-regulated kinase) and p38. Our results add novel insights to this contentious field.

Materials and methods

Cell cultures

Primary neonatal rat ventricular cardiomyocytes (R-CM-561) from Lonza (Lonza Walkersville, Inc. Walkersville, MD, USA) were plated at a density of 8×10^5 /100 mm plate and cultured, at 37°C in a 5% CO₂ humidified atmosphere, in Clonetics[®] RCGM Rat Cardiac Myocyte Growth Medium. Resv, Trolox, 6-chloro-2,3,4,9-tetrahydro-1H-carbazole-1-carboxamide (SIRT1 inhibitor), SB203580 (p38 kinase inhibitor), and PD98059 (MEK inhibitor), SP600125 (JNK inhibitor) were all purchased from Sigma (Sigma-Aldrich Co., St. Louis, MO). All other reagents were of the highest purity available.

Simulation of IR (ischemia–reperfusion)

Simulated IR was achieved using a modular incubator chamber (Billups-Rothenberg Inc., Del Mar, CA, USA), gassed with 95% NO₂ and 5% CO₂. A flow meter was used to measure the quantity of gas mixture introduced into the chamber (25 l/min), as shown by Namiki et al. [16]. To simulate IR, cells that had been incubated under conditions

of hypoxia in serum and in glucose-free medium for 5 h were reoxygenated by replacing the culture medium, and were returned to a normoxic environment at 37°C for 60 min. Cells were treated 24 h prior to hypoxic challenge by adding Resv or Trolox® at concentrations of 20 and 15 µM, respectively, which we found to display the same antioxidant capacity (see below). To check for possible toxic effects of these compounds, the normoxic control cardiomyocytes were also subjected to the same treatments. In another set of experiments, designed to determine the relative importance of ERK, p38 and JNK signaling pathways in this experimental model, cells were treated with 10 µM SB203580 (p38 kinase inhibitor), 10 µM SP600125 (JNK inhibitor) or 10 µM PD98059 (MEK inhibitor) for 1 h prior to hypoxia. In another set of experiments, 1 µM 6-chloro-2,3,4,9-tetrahydro-1H-carbazole-1-carboxamide (specific SIRT1 inhibitor) was added to the culture medium for 1 h prior to hypoxia.

Preparation of cell lysates

Cardiomyocytes were washed twice with phosphate buffered saline (PBS), trypsinized, centrifuged, and then resuspended in 100 µl of lysis buffer containing 1% Triton X-100, 20 mM Tris-HCl pH 8, 137 mM NaCl, 10% (v/v) glycerol, 2 mM EDTA, and 6 M urea supplemented with 0.2 mM PMSF, 10 µg/ml leupeptin, and aprotinin. To obtain cell lysates after three freeze-thaw cycles, cells were twice sonicated in ice for 5 s and then centrifuged at 14,000 × g for 10 min at 4°C. The supernatant was retained and protein concentration determined according to the Bradford method [17].

Measurement of lactate dehydrogenase release

Lactate dehydrogenase (LDH) activity, a marker of cell death, was assessed spectrophotometrically in culture medium and in adherent cells (in order to determine total LDH activity) using the LDH assay kit (Roche Diagnostics, Mannheim, Germany). LDH release was calculated as a percentage of total LDH content. In another set of experiments, designed to determine the relative importance of ERK, p38 and JNK signaling pathways in this experimental model, cells were treated with 10 µM SP600125 (specific JNK inhibitor), 10 µM PD98059 (MEK inhibitor) or 1 µM 6-Chloro-2,3,4,9-tetrahydro-1H-Carbazole-1-carboxamide (SIRT1 inhibitor) for 1 h prior to hypoxia.

Western-blot analysis of SIRT1, p-ASK1, p-ERK, and p-p38

To assess the levels of SIRT1, phosphorylated ERK (p-ERK) and phosphorylated p38 (p-p38), equal amounts

of cell lysates (40 µg for ERK1, p-ERK and SIRT1, 60 µg for p38 and p-p38) were diluted in Laemmli sample buffer, boiled for 5 min and separated on pre-cast 4–12% SDS-PAGE gels (Criterion XT, Bio-Rad, Hercules, CA). Proteins were blotted onto PVDF Hybond membranes, which were then incubated overnight at 4°C with (rabbit) anti-p-ASK1 pSer83 antibody (GenWay Biotech, Inc., San Diego, CA) (rabbit) anti-ASK1 (rabbit) anti-SIRT1 (rabbit) anti-ERK 1 (mouse) anti-p-ERK, (mouse) anti-p38 and (mouse) anti-p-p38 (Santa Cruz Biotechnology Inc., Santa Cruz, CA). After washing, the membranes were incubated with peroxidase-conjugated secondary antibodies for 1 h. Immunolabeled bands were detected using a supersignal west dura (Pierce, Rockford, IL, USA) and quantified using the aforementioned software for image analysis. Results were expressed as densitometric ratios between the protein of interest and the loading control (β -actin).

Immunoprecipitation and immunoblot analysis

For immunoprecipitation, whole cell lysates were pre-cleared with Protein A/G plus (Santa Cruz Biotechnology Inc.) for 30 min at 4°C. Beads were pelleted at 1,000 × g for 30 s and pre-cleared supernatants were incubated with 15 µg of primary antibody-agarose conjugates at 4°C overnight on a rotator. When agarose or a gel conjugate was unavailable, lysates were incubated with anti-Akt antibody (Santa Cruz Biotechnology Inc.) for 2 h at 4°C and then overnight along with Protein A/G plus beads to collect the immune complexes. Beads were collected by centrifugation, washed several times with RIPA buffer, one wash with PBS, and resuspended in SDS-PAGE sample loading buffer. Immune complexes and 80 µg of proteins were resolved by SDS-PAGE. Proteins were blotted onto PVDF Hybond membranes, which were then incubated overnight at 4°C with (mouse) anti-Akt antibody, (mouse) anti-pAkt (mouse) anti-Ac-lysine (Santa Cruz Biotechnology Inc.). After washing, the membranes were incubated with peroxidase-conjugated secondary antibodies for 1 h. Immunolabeled bands were detected using a supersignal west dura (Pierce, Rockford, IL, USA).

JNK levels

Cardiomyocytes were plated in 96-well culture plates and then subjected to the aforementioned procedure. After fixing cells in 4% formaldehyde (resuspended in PBS), total JNK and phosphorylated JNK were quantified using a commercially available assay (JNK ELISA kit; FACE, Active Motif Europe, Rixensart, Belgium), following the manufacturer's instructions.

Determination of intracellular ROS and mitochondrial superoxide

Cells were seeded on glass cover slips and loaded with the mitochondrial superoxide-specific fluorescent probe MitoSOX (3 μ M) and H₂DCFDA (2.5 μ M) (Invitrogen, CA, USA)—dissolved in 0.1% DMSO and pluronic acid F-127 (0.01% w/v), which was added to the cell culture media for 15 min at 37°C. Cells were fixed in 2.0% buffered paraformaldehyde for 10 min at room temperature and MitoSOX fluorescence analyzed (at an excitation wavelength of 514 nm) using a Leica TCS SP5 confocal scanning microscope (Leica, Mannheim, Germany) equipped with an argon laser for fluorescence analysis. A series of optical sections (1024 \times 1024 pixels) 1.0 μ m in thickness was taken through the cell depth at intervals of 0.5 μ m using a Leica 20 \times objective and then projected as a single composite image by superimposition.

H₂DCFDA fluorescence were analyzed (at an excitation wavelength of 488 nm) using a Leica TCS SP5 confocal scanning microscope (Mannheim, Germany) equipped with an argon laser for fluorescence analysis. A series of optical sections (1024 \times 1024 pixels) 1.0 μ m in thickness was taken through the cell depth at intervals of 0.5 μ m using a Leica plan apo 63 \times oil immersion objective and then projected as a single composite image by superimposition. ROS generation was also monitored by flow cytometry: single-cell suspensions were incubated with H₂DCFDA (1 μ M) (Invitrogen) for 15 min at 37°C and immediately analyzed.

Total antioxidant capacity (TAC)

Intracellular TAC, which accounts for ROS scavengers, was measured in cell lysates by chemiluminescent assay using the photoprotein Pholasin (Abel Antioxidant Test Kit, Knight Scientific Limited, Plymouth, UK), following the manufacturer's instructions. Protein content in the soluble fraction was measured using the Bradford method [17] and results were calculated using an L-ascorbic-acid-based standard curve.

Evaluation of lipid peroxidation

To assess the rate of lipid peroxidation, isoprostane levels were measured in cell lysates using the 8-isoprostane EIA kit (Cayman Chemical Co., Ann Arbor, MI, USA), following the manufacturer's instructions. Lipid peroxidation was also investigated by confocal scanning microscopy using BODIPY, a fluorescent probe that is intrinsically lipophilic and thus mimics the properties of natural lipids [18]. BODIPY 581/591 C11 acts as a fluorescent lipid peroxidation reporter that shifts its fluorescence from red to

green in the presence of oxidizing agents. Briefly, cells were cultured on glass cover slips and loaded with dye by adding the fluorescent probe BODIPY, dissolved in 0.1% DMSO (5 mM final concentration), to the cell culture media for 30 min at 37°C. The cells were fixed in 2.0% buffered paraformaldehyde for 10 min at room temperature and the BODIPY fluorescence was analyzed (at an excitation wavelength of 581 nm) using a confocal Leica TCS SP5 scanning microscope (Mannheim, Germany) equipped with an argon laser source for fluorescence measurements. A series of optical sections (1024 \times 1024 pixels) 1.0 μ m in thickness was taken through the cell depth at intervals of 0.5 μ m using a Leica plan apo 63 \times oil immersion objective and then projected as a single composite image by superimposition. Moreover, lipid peroxidation was quantified by flow cytometry. Single-cell suspensions were washed twice with PBS and incubated, in the dark, for 30 min at 37°C with BODIPY 581/591 (2 mM) in DMEM. After labeling, cells were washed and resuspended in PBS and analyzed using a FACSCanto flow cytometer (Becton-Dickinson, San Jose, CA, USA).

Mitochondrial number

Mitochondrial number was determined using mitotracker deep red 633 (Invitrogen), which was used to stain mitochondria, and confocal microscopy used to visualize individual mitochondria. Briefly, cells were seeded on glass cover slips and loaded with mitotracker deep red 633 fluorescent probe (0.5 μ M)—dissolved in 0.1% DMSO and pluronic acid F-127 (0.01% w/v), which was added to cell culture media for 20 min at 37°C. Cells were fixed in 2.0% buffered paraformaldehyde for 10 min at room temperature and red fluorescence analyzed (at an excitation wavelength of 633 nm) using a Leica TCS SP5 confocal scanning microscope (Mannheim, Germany) equipped with an argon laser source for fluorescence analysis. Mitochondrial number was also monitored by flow cytometry. Single-cell suspensions were incubated with mitotracker deep red 633 (200 nM) for 20 min at 37°C and immediately analyzed by flow cytometry.

Mitochondrial permeability transition pore opening

Mitochondrial permeability was analyzed using the fluorescent calcein-AM probe, according to the method described by Petronilli et al. [19], albeit with minor modifications. Calcein-AM freely enters cells and emits fluorescence upon de-esterification. Co-loading of cells with cobalt chloride quenches cell fluorescence except in mitochondria. This is because cobalt cannot cross mitochondrial membranes (living cells). During mitochondrial permeability transition pore opening (mPTP), cobalt can

enter mitochondria and is able to quench calcein fluorescence (apoptotic cells). Thus, decreased mitochondrial calcein fluorescence can be considered a measure of the extent of mPTP induction. Briefly, single-cell suspensions were incubated with the fluorescent probes calcein-AM (Invitrogen) (3 μ M) and cobalt chloride (1 mM) for 20 min at 37°C, washed twice with PBS and analyzed using a FACSCanto flow cytometer (Becton-Dickinson, San Jose, CA, USA).

Assessment of caspase activity by FACS analysis

Caspase-3 and caspase-9 activity was analyzed by flow cytometry. In brief, single-cell suspensions were incubated with FAM-FLICA™ Caspases solution (Caspase FLICA kit FAM-DEVD-FMK) for 1 h at 37°C, washed twice with PBS and analyzed using a FACSCanto flow cytometer (Becton-Dickinson). In another set of experiments, designed to determine the relative importance of ERK, p38 and JNK signaling pathways in this experimental model, cells were treated with 10 μ M SP600125 (specific JNK inhibitor), 10 μ M PD98059 (MEK inhibitor) or 1 μ M SIRT1 inhibitor for 1 h prior to hypoxia.

Mitochondrial membrane potential

Mitochondrial membrane potential was assessed using tetramethylrhodamine methyl ester perchlorate (TMRM) (Invitrogen). TMRM is a lipophilic potentiometric dye that partitions between the mitochondria and cytosol in proportion to mitochondrial membrane potential ($\Delta\psi$), by virtue of its positive charge. At low concentrations, fluorescence intensity is a function of dye concentration, which is in turn a direct function of mitochondrial potential. Therefore, the accumulation of dye in mitochondria and the intensity of the signal is a direct function of mitochondrial potential. Mitochondrial membrane potential was also quantified by flow cytometry. Single-cell suspensions were washed twice with PBS and then incubated, in the dark, for 20 min at 37°C with TMRM (100 nM) resuspended in DMEM. After labeling, the cells were washed and resuspended in PBS, and analyzed using a FACSCanto flow cytometer.

Determination of cellular SIRT1 activity

Cellular SIRT1 activity was determined according to the method described by Fulco et al. [20] with some modifications. Cell extracts were obtained by using a lysis buffer (50 mM Tris-HCl pH 8, 125 mM NaCl, 1 mM DTT, 5 mM MgCl₂, 1 mM EDTA, 10% glycerol, and 0.1% NP40 supplemented with 1 mM PMSF and protease

inhibitors mix) and SIRT1 activities were determined by SIRT1 direct fluorescent screening assay kit (Cayman, Ann Arbor, MI). A total of 25 μ l of assay buffer (50 mM Tris-HCl, pH 8.0, containing 137 mM NaCl, 2.7 mM KCl, and 1 mM MgCl₂), 5 μ l of extracts, and 15 μ l of substrate solution were added to all wells. The plate was incubated on a shaker for 45 min; 50 μ l of stop/development solution was added to each well and incubated for 30 min at room temperature. The fluorescence of the plate was then determined using a Perkin-Elmer LS 55 luminescence spectrometer using as excitation wavelength of 360 nm and an emission wavelength of 460 nm.

Statistical analysis

All data is expressed as mean \pm SD. Comparisons between different groups were carried out using the one-way analysis of variance (ANOVA) followed by Bonferroni *t* test. A *p* value of <0.05 was accepted as statistically significant.

Results

Dose-dependent effects of Resv on SIRT1 expression and activity

As a preliminary test aimed at evaluating the effect of Resv on SIRT1 expression, dose-dependent Western-blot analysis of cell lysates was carried out in the presence of increasing Resv concentrations (from 2.5 μ M to 40 μ M). Cardiomyocytes subjected to 24 h-treatment with 20 μ M Resv displayed a 3.5-fold increase in SIRT1 expression (Fig. 1a). We also tested the effect of Resv in modulating SIRT1 activity in the presence of the same increasing Resv concentrations. Cardiomyocytes subjected to 24-h treatment with 20 μ M Resv displayed a fourfold increase in SIRT1 activity (Fig. 1b).

Effects of Resv and Trolox on control cells

In order to verify the possible direct effect of Resv and Trolox on the considered parameters, independent of IR conditions, these substances were added, at the same concentrations used to treat IR cells, to control normoxic neonatal rat ventricular cardiomyocytes. No significant changes were observed in control cells, except for expected increases in TAC, exerted by the two antioxidants (Table 1) and in SIRT1 expression, displayed by Resv (Fig. 3). SB203580, SP600125, and SIRT1 inhibitor, when added to control cells at the same concentration used during experiments, caused no toxic effects (data not shown).

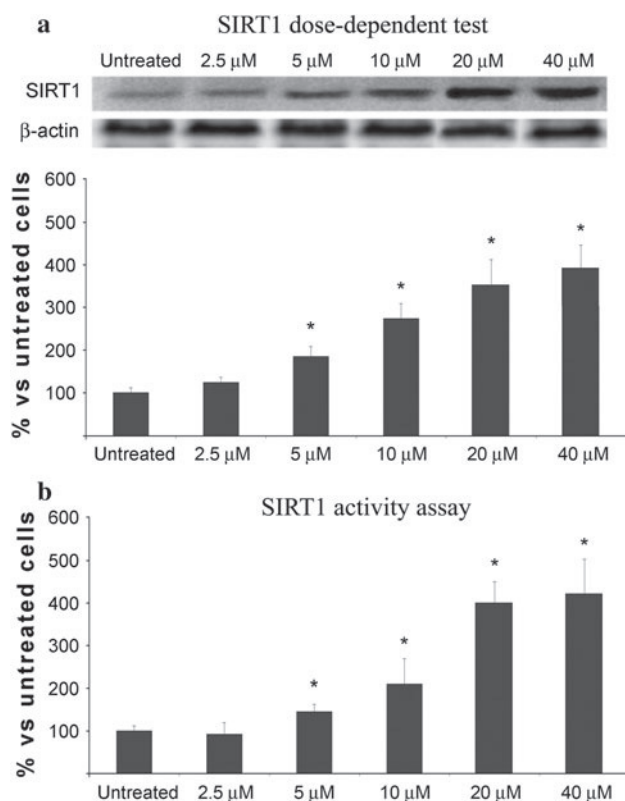


Fig. 1 SIRT1 expression (a) and activity (b) in neonatal rat ventricular cardiomyocytes after 24 h of incubation with different concentrations of Resv. In Western-blot analysis, all signals were quantified by densitometric analysis and are expressed as ratio of SIRT1 densitometry on β -actin (loading control) densitometry. *Significant difference ($p \leq 0.05$) versus untreated cells. The reported values (mean \pm SD) are representative of four independent experiments, each performed in triplicate

Oxidative stress markers and antioxidant protection of SIRT1 overexpression in neonatal cardiomyocytes subjected to simulated IR

To investigate the effect of SIRT1 overexpression, neonatal rat ventricular cardiomyocytes were grown for 24 h in the presence of 20 μ M Resv. To see whether the effects of Resv were due to its antioxidant activity only, experiments were also performed in the same cells treated with 15 μ M Trolox, a concentration required to obtain the same antioxidant capacity (assayed as above described) of 20 μ M Resv. TAC and lipoperoxidation markers (8-isoprostane levels and BODIPY fluorescence) were measured in these cells (Table 1; Fig. 2d). Compared to controls, IR cells exhibited marked reduction in TAC and a significant increase in the concentration of 8-isoprostanes confirming the results of our previous investigation [21]. All cells treated with Resv and Trolox (both without and with IR) displayed significantly higher TAC with respect to corresponding untreated cells ($p < 0.05$); treatment with Resv caused a significant increase in cellular TAC after IR

injury, more so than Trolox. As with the increased TAC, the concentration of 8-isoprostanes was much lower in Resv-treated IR cells compared to Trolox-treated IR cells ($p < 0.05$). ROS production was investigated by FACS and confocal microscopy analysis using the fluorescent probe H_2DCFDA (Fig. 2a, b). IR cells produced intense fluorescent signals, indicating a strong and significant increase in ROS production. Resv- and Trolox-treated IR cells were characterized by less-marked fluorescence, demonstrating a strong protective effect of these compounds against ROS production. Similar results were obtained evaluating mitochondrial superoxide production by confocal microscope analysis (Fig. 2c). Resv again proved to be more protective than Trolox. In the presence of SIRT1 inhibitor, the intensity of ROS production did not differ significantly from untreated IR cardiomyocytes.

SIRT1 expression and activity in IR cardiomyocytes

The effect of Resv on SIRT1 expression and activity under conditions of oxidative stress were investigated. As shown in Fig. 3a, when cells were subjected to simulated IR the expression of endogenous SIRT1 was only slightly, but significantly, increased (+25% vs. control, $p < 0.05$). Interestingly, pre-treating with Resv upregulated SIRT1 expression (+150% vs. control, $p < 0.05$): similar pre-treatment with Trolox did not, however (NS vs. control). However, a significant decrease in SIRT1 expression was observed upon addition of a SIRT1 inhibitor to Resv-pre-treated cells ($p < 0.05$ vs. control, $p < 0.05$ vs. IR). Also, as shown in Fig. 3b, SIRT1 activity was significantly increased in IR condition (+50% vs. control, $p < 0.05$) and pre-treating with Resv upregulated SIRT1 activity (+300% vs. control, $p < 0.05$). Trolox treatment did not affect SIRT1 activity in IR condition.

Resv-induced SIRT1 overexpression protects cardiomyocytes from IR-induced necrosis and apoptosis

Necrotic cell death in IR neonatal rat cardiomyocytes was assessed by measuring LDH release (LDH released/total LDH). Our results (Fig. 4a) show that IR induced about ten-fold increase in cell death compared to control cells ($p < 0.05$). Trolox treatment triggered a significant decrease in the rate of cell death (-28% vs. IR, $p < 0.05$). An even more protective effect was exerted by Resv, which, compared to IR cells, reduced cell death by half ($p < 0.05$ vs. IR, $p < 0.05$ vs. Trolox). Interestingly, cells treated with both Resv and a SIRT1 inhibitor displayed higher levels of cell death to those observed in IR cells ($p < 0.05$ vs. IR).

Table 1 Redox status in neonatal rat ventricular cardiomyocytes

	Total antioxidant capacity ascorbate equivalent unit (nmol/mg of protein)	8-Isoprostanes (pg/mg of protein)
Control	14.01 ± 1.52	55.42 ± 5.61
Control + Trolox	21.70 ± 2.01*	59.04 ± 6.21
Control + resveratrol	22.54 ± 2.13*	51.80 ± 5.43
Control + resveratrol + SIRT1 inhibitor	9.48 ± 0.80*	49.43 ± 5.65
IR	10.46 ± 0.93*	244.58 ± 15.30*
IR + Trolox	14.18 ± 1.04 [#]	132.53 ± 11.75 [#]
IR + resveratrol	21.44 ± 2.34 [#]	81.95 ± 7.29 [#]
IR + resveratrol + SIRT1 inhibitor	10.9 ± 1.21*	208.41 ± 22.14 [#]

Cellular TAC (total antioxidant capacity) and lipid peroxidation levels (8-isoprostanes) measured in the cytosolic fractions of neonatal rat ventricular cardiomyocytes

* Significant difference ($p \leq 0.05$) versus control (C) cells. [#]Significant difference ($p \leq 0.05$) versus IR cells

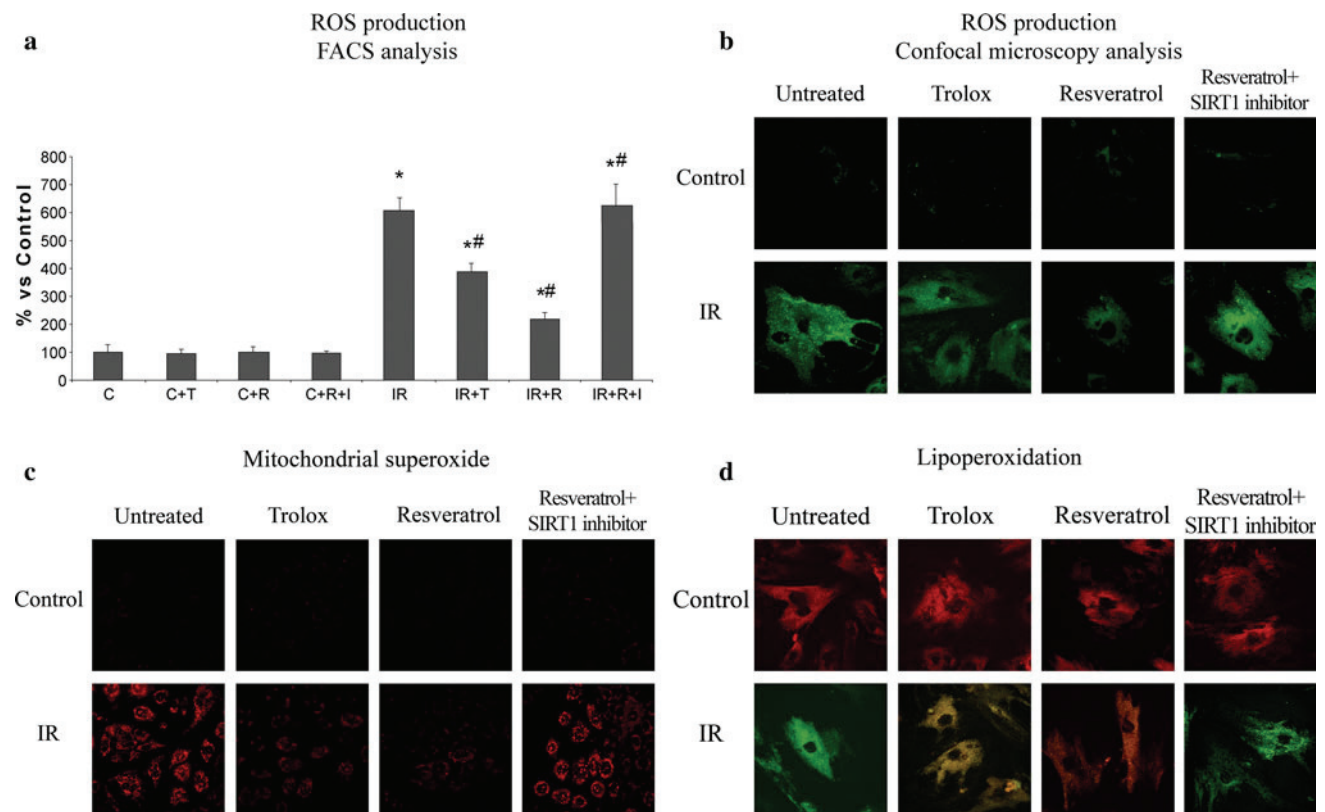


Fig. 2 **a** FACS analysis of ROS production by H₂DCFDA fluorescence in control normoxic (C) and in IR neonatal rat ventricular cardiomyocytes in the presence of Resv (R), Trolox (T), or SIRT1 inhibitor (I). *Significant difference ($p \leq 0.05$) versus control (C) cells. [#]Significant difference ($p \leq 0.05$) versus IR cells.

b Confocal microscope analysis of ROS production (63× magnification). **c** Mitochondrial superoxide (20× magnification), and **d** lipoperoxidation (63× magnification) in IR neonatal rat ventricular cardiomyocytes. The reported values (mean ± SD) are representative of five independent experiments, each performed in triplicate

Caspase-3 and -9 activities were measured to confirm that apoptosis occurs under our experimental conditions and to explore a potential correlation with SIRT1 activation. As shown in (Fig. 4b, c) an increase in caspase-3 and caspase-9 activities was seen in ischemic cells following

1 h of reperfusion (both caspase-3 and caspase-9 activities were about fourfold higher compared to controls; $p < 0.05$). This increase was reversed by Resv pre-treatment prior to ischemic challenge (both for caspase-3 and caspase-9, Resv vs. IR $p < 0.05$). Trolox, albeit to a lesser

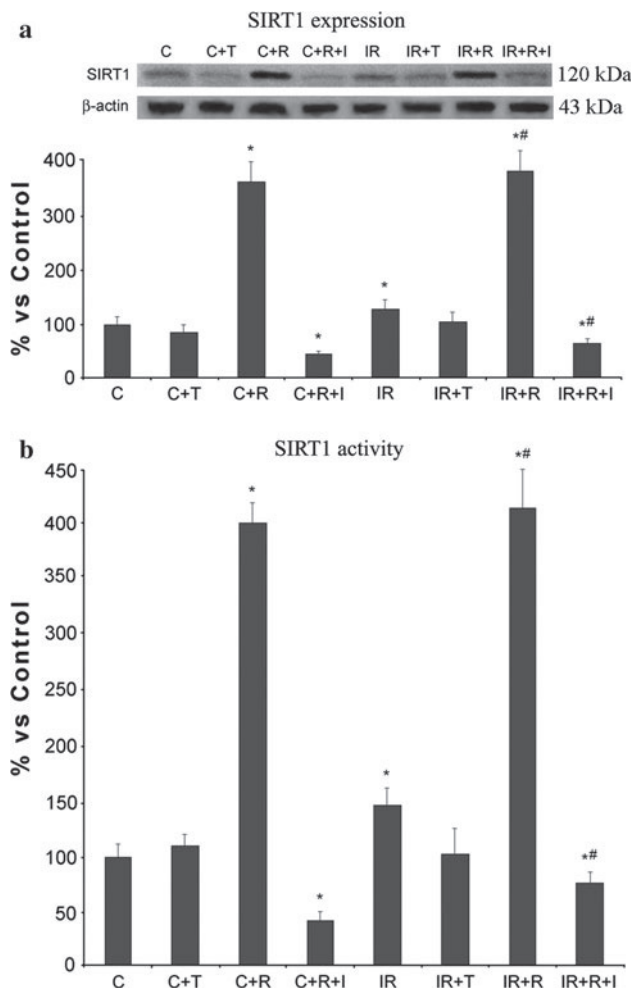


Fig. 3 SIRT1 expression **a** and activity **b** in IR neonatal rat ventricular cardiomyocytes. In western blot analysis all signals were quantified by densitometric analysis and were expressed as a ratio of SIRT1 densitometry versus β -actin (loading control) densitometry. *Significant difference ($p \leq 0.05$) versus untreated cells. #Significant difference ($p \leq 0.05$) versus IR cells. Control normoxic cells (C), Resv (R), Trolox (T), SIRT1 inhibitor (I). The reported values (mean \pm SD) are representative of four independent experiments, each performed in triplicate

extent, significantly reduced apoptosis (both for caspase-3 and caspase-9 Trolox vs. IR $p < 0.05$). In any case, a significant difference ($p < 0.05$) was observed between Resv and Trolox treatments, both for caspase-3 and caspase-9. In IR cells, a significant increase in caspase-3 and -9 activities was evident when SIRT1 inhibitor was added to the reaction medium.

To further investigate the observed protective effect, we explored, in IR cardiomyocytes, in the presence of Resv, Trolox or Resv and SIRT1 inhibitor, mitochondrial depolarization and mitochondrial permeability transition pore opening (Fig. 5a, b), which are usually considered markers of cell suffering and apoptosis.

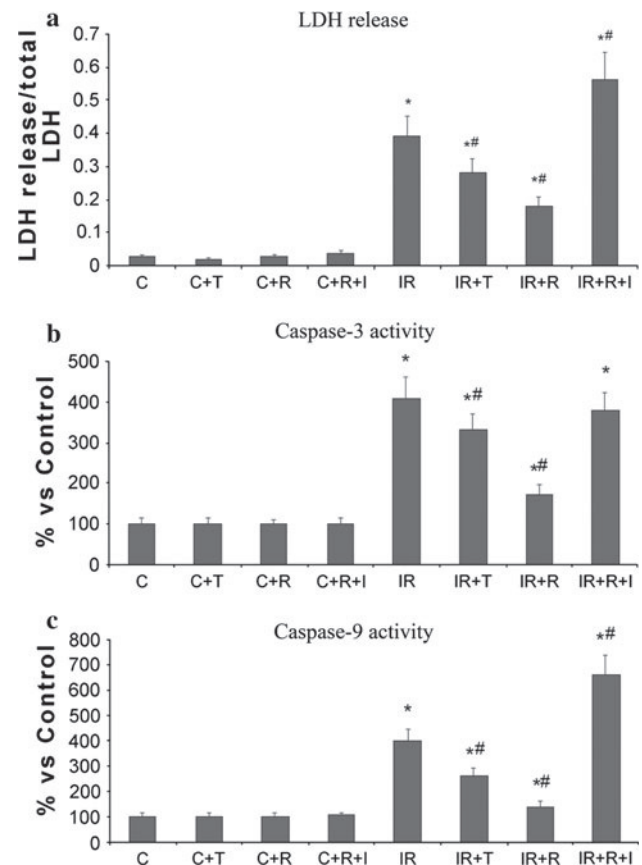


Fig. 4 **a** Release of cellular LDH into the culture media measured by spectrofluorimetric analysis, **b** the caspase-3, and **c** caspase-9 activities measured by flow cytometry assayed in IR neonatal rat ventricular cardiomyocytes. *Significant difference ($p \leq 0.05$) versus control cells. #Significant difference ($p \leq 0.05$) versus IR cells. Control normoxic cells (C), Resv (R), Trolox (T), SIRT1 inhibitor (I). The reported values (mean \pm SD) are representative of four independent experiments, each performed in triplicate

As expected, simulated IR strongly impaired mitochondrial depolarization (Fig. 5a), which was restored upon Resv treatment ($p < 0.05$ vs. untreated IR), and to a lesser extent by Trolox ($p < 0.05$ vs. untreated IR). Treating IR cells with both Resv and SIRT1 inhibitor did not cause any significant change compared to untreated IR cells. Similar effects were observed when assessing mitochondrial permeability transition pore opening (Fig. 5b), which was markedly affected by IR and efficiently restored by Resv treatment only ($p < 0.05$ vs. untreated IR).

Mitochondrial number can influence experiments where mitochondrial function is investigated; we therefore counted the number of mitochondria in Resv-treated or not-treated neonatal cardiomyocytes to ensure that increased mitochondrial function was not due to increased mitochondrial number. In our experimental conditions, there was no significant increase in mitochondrial number upon Resv treatment (data not shown). Therefore, the observed

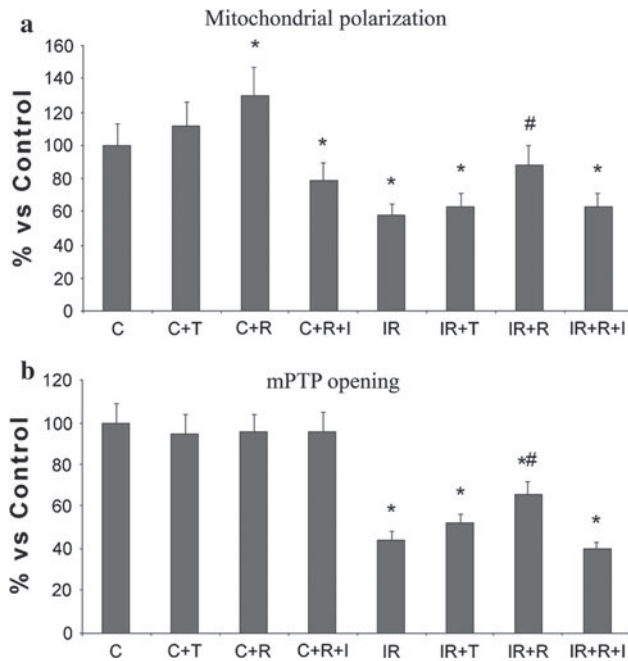


Fig. 5 **a** Mitochondrial depolarization and **b** mitochondrial permeability transition pore opening measured by flow cytometry in IR neonatal rat ventricular cardiomyocytes. *Significant difference ($p \leq 0.05$) versus control cells. #Significant difference ($p \leq 0.05$) versus IR cells. Control normoxic cells (C), Resv (R), Trolox (T), SIRT1 inhibitor (I). The reported values (mean \pm SD) are representative of four independent experiments, each performed in triplicate

changes in mitochondrial function and cell viability were not due to changes in mitochondrial number.

MAPK pathways are affected by Resv treatment in IR cardiomyocytes

As shown previously, neonatal cardiomyocytes subjected to simulated IR showed signs of oxidative stress and cell death. To investigate the pathways involved in cell damage, we examined p38, ERK, and JNK activation, all of which are regulated by redox status. Under our experimental conditions, simulated IR induced an almost twofold increase in the p-p38/total p38 ratio (Fig. 6a) ($p < 0.05$ vs. control), p38 being an enzyme whose activation is associated with the triggering of apoptosis. Resv treatment reduced p38 phosphorylation to control levels (NS vs. control, $p < 0.05$ vs. IR). Treatment with Trolox or with Resv + SIRT1 inhibitor did not lead to a similar reduction in p-38 phosphorylation (NS vs. IR).

The levels of JNK phosphorylation are shown in Fig. 6b. Simulated IR led to an increase in the p-JNK/total JNK ratio, which was significant compared to controls ($p < 0.05$). As already observed, Resv significantly decreased the entity of JNK phosphorylation ($p < 0.05$ vs. IR).

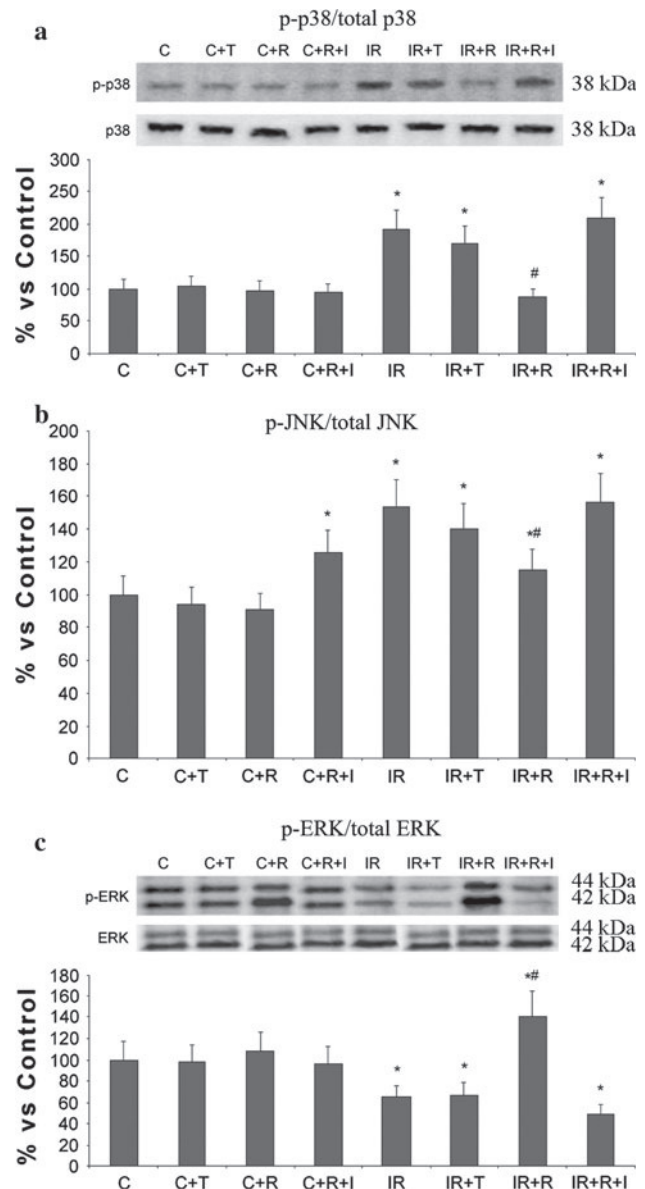


Fig. 6 MAPK phosphorylation in IR neonatal rat ventricular cardiomyocytes. **a** Western-blot analysis of phosphorylated p38 expression. All signals were quantified by densitometric analysis and were expressed as a ratio of p-p38 densitometry versus total p38 (loading control) densitometry. **b** Quantification of total and phosphorylated c-Jun N-terminal kinase by ELISA. **c** Western-blot analysis of phosphorylated ERK expression. All signals were quantified by densitometric analysis and were expressed as a ratio of p-ERK densitometry versus total ERK (loading control) densitometry. *Significant difference ($p \leq 0.05$) versus control cells. #Significant difference ($p \leq 0.05$) versus IR cells. Control normoxic cells (C), Resv (R), Trolox (T), SIRT1 inhibitor (I). The reported values (mean \pm SD) are representative of four independent experiments, each performed in triplicate

Figure 6c shows the levels of ERK phosphorylation, whose anti-apoptotic effect is well documented. In this case, simulated IR lead to a significant reduction in the

p-ERK/total ERK ratio, which was reversed by Resv treatment only ($p < 0.05$ vs. IR).

To probe the possible relationships between SIRT1 and MAPK pathways in IR, we analyzed caspase-3 activity and LDH release in the presence of specific MAPK and SIRT1 inhibitors. As previously described, IR triggered a marked increase ($p < 0.05$ vs. control) in caspase-3 activity (Fig. 7a). Pre-treating cells with Trolox or Resv caused a sharp reduction in caspase-3 activation ($p < 0.05$ vs. untreated IR). When SIRT1 inhibitor was used, caspase-3 activity rose to values similar to those seen in untreated IR cells (NS vs. IR). In the presence of p38 or JNK inhibitor (p38i or JNKi, respectively), levels of apoptosis significantly decreased ($p < 0.05$ vs. untreated IR), suggesting the involvement of these pathways in IR-induced cell death. When Resv was added along with these inhibitors, caspase-3 activity further decreased ($p < 0.05$ vs. IR + p38i or JNKi). The presence of SIRT1 inhibitor together with p38i or JNKi triggered an increase in caspase-3 activity (NS vs. IR + p38i or JNKi). Interestingly, IR cells displayed the greatest caspase-3 activity in the presence of ERK inhibitor. Caspase-3 activity was unaffected by other treatments, thus suggesting a prominent role for ERK in protection against apoptotic cell death. When LDH release was assayed in the presence of antioxidants and p38, JNK, and ERK inhibitors (Fig. 7b), maximum LDH release was again observed in the presence of the ERK inhibitor. Pre-treatment with p38 and JNK inhibitors clearly protected against cell death, as shown by the decrease in LDH release. Simultaneous treatment with the three inhibitors did not protect against cell death (data not shown). When antioxidants were added along with p38 or JNK inhibitor, treatment with Trolox led to a mild decrease in LDH. The decrease in LDH release was more marked following treatment with Resv, however, indicating greater protection against cell death. In the presence of ERK, inhibitor antioxidants did not protect against necrotic cell death, indicating a crucial role for this pathway in preventing IR-induced cell death.

SIRT1 deacetylates Akt and inhibits ASK1 activation

To identify the potential intermediates between SIRT1 and MAPKs pathways, we examined Akt (protein kinase B) and apoptosis signal-regulating kinase 1 (ASK1) that acts upstream of JNK and p38 kinases [22, 23]. Deacetylation of lysine residues is a posttranslational mechanism that controls the activity of many cellular proteins, including kinases. It has been shown that SIRT1 activate Akt and that Akt can phosphorylate ASK1 at Ser-83 to maintain ASK1 in an inactive form [24]. Akt immunoprecipitates from cardiomyocytes indicated that phosphorylation of Akt was enhanced in Resv-treated cells, findings that were

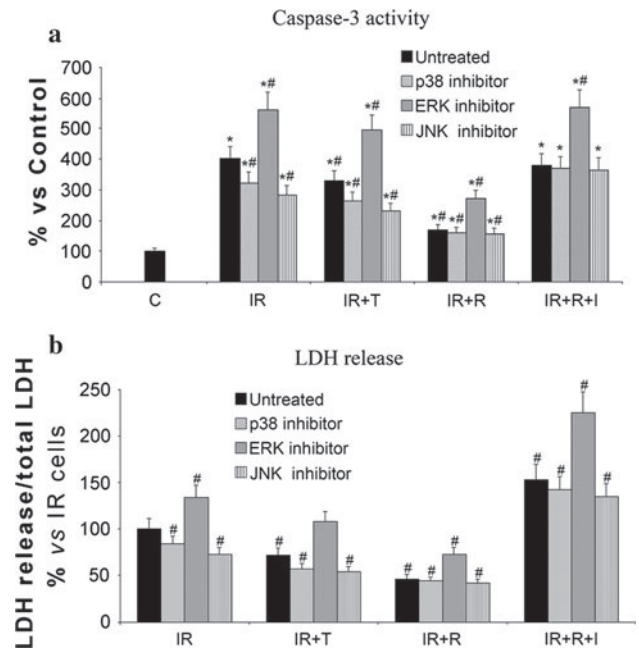


Fig. 7 **a** Caspase-3 activity measured using flow cytometry and **b** the release of cellular LDH into the culture media assayed in IR neonatal rat ventricular cardiomyocytes in the presence of specific MAPK inhibitors. *Significant difference ($p \leq 0.05$) versus control cells. #Significant difference ($p \leq 0.05$) versus IR cells. Control normoxic cells (C), Resv (R), Trolox (T), SIRT1 inhibitor (I). The reported values (mean \pm SD) are representative of four independent experiments, each performed in triplicate

associated with Akt deacetylation, indicating that SIRT1 deacetylates and activates Akt (Fig. 8a). Interestingly, when SIRT1 inhibitor was used, deacetylation and phosphorylation level of Akt decreased to values similar to those seen in untreated IR cells, demonstrating that SIRT1 is necessary for Akt activation. Furthermore, phosphorylation level at Ser-83 of ASK1 (a specific Akt phosphorylation site) was high in Resv-treated cardiomyocytes indicating that Akt can inactivate ASK1 via SIRT1 pathways (Fig. 8b). When SIRT1 inhibitor was added, ASK1 phosphorylation level at Ser-83 greatly decreased.

Discussion

Myocardial IR injury is an important cause of organ damage. Reperfusion triggers a series of adverse events that culminate in contractile dysfunction, endothelial dysfunction, and cell death [25, 26]. There are currently no drugs for clinical use to reduce reperfusion injury, indeed, the pathways implicated in IR injury are the subject of intense research.

In the present study, neonatal rat cardiomyocytes, subjected to simulated IR, exhibited marked biochemical changes, including clear signs of oxidative stress (increase

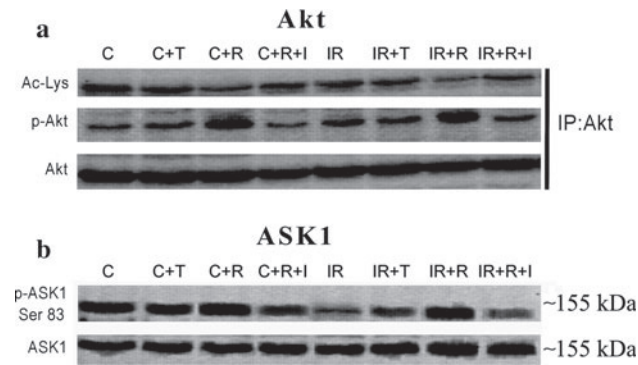


Fig. 8 **a** The phosphorylation and acetylation status of Akt immunoprecipitated from neonatal rat ventricular cardiomyocytes determined by immunoblotting. **b** Western-blot analysis of ASK1 phosphorylation at Ser83 in neonatal rat ventricular cardiomyocytes. Control normoxic cells (C), Resv (R), Trolox (T), SIRT1 inhibitor (I). The reported values (mean \pm SD) are representative of four independent experiments, each performed in triplicate

in ROS production and in lipoperoxidation markers) and cell death (both apoptosis and necrosis). Mitochondrial dysfunction appeared to play a prominent role in ROS production and in the onset of oxidative stress in general: indeed, mPTP opening and aberrant mitochondrial depolarization were associated with significantly higher mitochondrial superoxide generation.

The combined increase in ROS generation and depletion of antioxidant defenses during IR results in oxidative modification of biomolecules. Protein oxidation, which is particularly damaging in the electron transport chain, causes structural changes that impair mitochondrial respiration and ATP synthesis [27]. IR neonatal cardiomyocytes displayed elevated levels of 8-isoprostanes (an index of lipoperoxidation) and a marked reduction in total antioxidant capacity, consistent with the results we obtained in a previous study [21]. Confocal microscope analysis revealed high levels of mitochondrial superoxide following reperfusion. Resv- and Trolox-treated IR cells were characterized by a reduction in ROS production and in isoprostane levels and by an increase in the overall antioxidant defense system, demonstrating a strong protective effect of these compounds. Interestingly, in our study, we used Trolox and Resv at the same antioxidant capacity (as assessed by luminometric assay (data not shown) to determine whether the effects of these compounds were simply a function of their antioxidant activity. Interestingly, Resv proved to be more protective (as suggested by the sharp reduction in oxidative stress markers, LDH release and caspase activities) compared to Trolox, an effect that is correlated with SIRT1 overexpression.

These findings agree with the reported Sirt1-induced resistance to oxidative stress through FoxO in fibroblasts [4]. In this study, overexpression of either Sirt1 or

constitutively active FoxO1a in cultured cardiac myocytes stimulated expression of catalase, whereas upregulation of catalase was inhibited in the presence of dominant negative FoxO1a.

In our study, simulated IR caused strong impairment of mitochondrial depolarization, which was restored by Resv treatment and, to a lesser extent, by Trolox. We observed similar effects when assessing mitochondrial permeability transition pore opening, which was markedly affected by IR and fully restored by Resv treatment only. All the above protective effects against cellular injury induced by IR were evident in Resv-treated IR ventricular myocytes, which displayed a twofold increase in SIRT1 expression compared to untreated IR cells.

In the presence of SIRT1 inhibitor, the protective effects of Resv on IR-induced cell death parameters (particularly caspase activity and LDH release) were completely abolished, indicating a prominent role for SIRT1 in this process.

These results agree with recent findings indicating that Resv attenuates both steady-state and high glucose-induced mitochondrial ROS production in cultured human coronary arterial endothelial cells (CAECs). Similar effects, in the same cells, were observed by SIRT1 overexpression, thus mimicking Resv treatment and were attenuated by SIRT1 knockdown [28].

Our data clearly show that IR triggers necrotic cell death. While Trolox treatment significantly slowed the rate of necrosis, Resv exerted a more marked effect, highlighting the protective effect of SIRT1 overexpression also in IR-induced necrosis. Interestingly, cells treated with both Resv and a SIRT1 inhibitor displayed levels of cell death fourfold higher than Resv-treated IR cardiomyocytes and, however, higher than untreated IR cells.

Caspase-3 and caspase-9, which play a key role in apoptotic cell death, displayed increased activity in ischemic cells following 1 h of reperfusion. Pre-treating cells with Resv prior to ischemic challenge precluded this increase. Treatment with Trolox, albeit to a lesser extent, also promoted a significant reduction in apoptotic cell death. The presence of SIRT1 inhibitor together with Resv counteracted this reduction. In this case, caspase-3 and -9 activities did not differ significantly from IR cardiomyocytes, suggesting that Resv may exert its anti-apoptotic effects via SIRT1. The fact that SIRT1 inhibition abolished the protective effects of Resv suggests that SIRT1 activation plays a fundamental role in Resv-induced cardioprotection during IR.

Recently, several authors reported that sirtuins may play a role in cardioprotection and cardiac hypertrophy. Pharmacological studies have shown that SIRT1 overexpression protects cardiomyocytes from serum deprivation-induced death [12]. In contrast, sirtuin knockdown triggered cell

death in isolated neonatal rat cardiomyocytes [29]. It was shown that Resv protects H9c2 cells from hypoxia-induced apoptosis by signaling via the SIRT1-FOXO1 pathway [15]. Moreover, SIRT1-induced upregulation of antioxidants and downregulation of pro-apoptotic molecules, via FOXO activation and reduction of oxidative stress, protecting transgenic mice from IR-induced cardiac injury [30].

Indeed, our findings suggest that SIRT1 expression is upregulated by IR. Consistent with this, other authors suggested that SIRT1 expression was upregulated by cardiac stressors, including oxidative stress, aging, and heart failure [4, 12], helping protect the heart from damage. Together with previous evidence of its cardioprotective role in the aging process and in oxidative stress [4], our results suggest that stimulation of SIRT1 may represent a novel approach to protect the heart from ischemic injury. Indeed, our findings suggest that SIRT1 expression is upregulated by IR. Consistent with this, SIRT1 expression was also found to be upregulated by other cardiac stressors, including oxidative stress, aging, and heart failure [4, 12], helping protect the heart from damage. The regulation of SIRT1 expression therefore appears stimulus-specific. In animal models, Resv protects cardiac tissue from IR injury [14]. Although Resv can stimulate both SIRT1 and SIRT3, whether SIRT1 activation is brought about by direct interaction between the two molecules, or via intermediates, remains to be determined [31]. Resv could also exert its cardioprotective effects—such as its antioxidant role—via SIRT1-independent mechanisms [32]. Our findings suggest that SIRT1 overexpression protects against IR injury. Importantly, Resv only promotes lifespan extension when the SIR2 gene is present, having no effect when the gene is deleted [33]. Resv treatment prevented IR-induced cell death and enhanced SIRT1 activity, which was maintained post-IR. However, the fact that SIRT1 inhibition abolished the protective effects of Resv suggests that SIRT1 activation plays a fundamental role in Resv-induced cardioprotection during IR.

A recent study by Hsu and colleagues found that SIRT1 upregulates the expression of cardioprotective molecules, such as MnSOD, Trx1, and Bcl-xL, and at the same time downregulates pro-apoptotic molecules, including Bax [30]. SIRT1 is also known to deacetylate FOXO, leading to upregulated expression of genes involved in cell-protective processes [34]. Indeed, upregulation of MnSOD expression by SIRT1 (as observed in cultured cardiomyocytes, for example) seems tightly regulated by FOXO1.

In the cardiovascular system, Akt (protein kinase B) plays critical roles in the regulation of cardiac hypertrophy, angiogenesis, and apoptosis [35]. In cardiomyocytes, activation of the Akt pathway by insulin-like growth factor 1 (IGF-I) appears to be necessary for the anti-apoptotic

effects of IGF-I [36] and adenoviral expression of constitutively active mutants of Akt reduces hypoxia-induced apoptosis *in vitro*, while inhibition of Akt activity accelerated hypoxia-induced cardiomyocyte dysfunction [37]. Akt activity is also involved in ischemia/reperfusion-induced myocardial injury and Akt activation accounts for cardioprotection in rat heart [38–40].

Phosphorylation of residues Thr-308 and Ser-473 is required for Akt activity [24, 41, 42]. Active Akt phosphorylates BAD, caspase-9, glycogen synthase kinase 3 (GSK-3), ASK1, fork-head transcription factors, and thereby induces antiapoptotic effects [24, 41].

Deacetylation of lysine residues by histone deacetylases is a posttranslational mechanism that controls the activity of many cellular proteins, including kinases [43, 44]. SIRT1 regulates many of the same cellular processes regulated by Akt [44], and SIRT1 activators have been used to treat metabolic disorders characterized by defective Akt signaling [45]. A recent study of Sundaresan and coworkers [46] demonstrated that Akt deacetylation by SIRT1 is a necessary mechanism for its activation. Here, we confirm that SIRT1 promotes Akt activation in our cellular model and protects cardiomyocytes from IR-induced cell death.

Apoptosis signal-regulating kinase 1 (ASK1) represents a mitogen-activated protein kinase kinase kinase family member that acts upstream of JNK and p38 kinases [22, 23]. A number of studies have shown that ASK1 is activated by a variety of stress-related stimuli, including serum withdrawal, ROS, TNF- α , and IR [47, 48]. Phosphorylation of ASK1 at Ser-83 (a specific Akt phosphorylation site) is correlated with the decreased activity of ASK1. It has been shown that Akt can phosphorylate ASK1 at Ser-83 to maintain ASK1 in an inactive form, however, Thr-845 is an autophosphorylation site that is critical for ASK1 activation [24, 49].

In our present study, we examined the activity of ASK1 in IR. As shown in Fig. 8, we found that the phosphorylation of ASK1 at Ser-83 was diminished and at the same time, the phosphorylation of JNK and p38 dramatically increased. It has been reported that H₂O₂ can induce the decreased phosphorylation of Akt and ASK1 (Ser-83), while the phosphorylation of ASK1 at Thr-845 was increased. Akt, however, had little effect on the H₂O₂ responsiveness of the ASK1 point mutant, ASK1S83A, suggesting a specific phosphorylation event in Akt-mediated inhibition [42]. Our findings indicate that ASK1 is activated in response to IR and Resv treatment increased ASK1 phosphorylation at Ser-83 to control levels.

Myocyte apoptosis is induced during reperfusion by activating pro-injurious kinases, including p38-mitogen-activated protein kinase (MAPK) and c-jun NH₂-terminal kinase (JNK) [50] whose induction by physical, chemical, and physiological stressors [3] is well documented.

In contrast, cardioprotection is afforded by activating extracellular regulated kinase (ERK1/2) and AKT [51, 52]. In this study, the effect of SIRT1 overexpression in relation to MAPK signaling in IR ventricular myocytes was examined. JNK, ERK-1/2, and p38 kinases showed opposing regulatory effects on apoptosis. Using specific inhibitors for each MAPK sub-type, we demonstrated that JNK and p38 kinases exerted pro-apoptotic effects, whereas ERK was anti-apoptotic and therefore protected against IR-induced apoptosis. Numerous studies have shown that activation of ERK signaling by various stimuli has a cardioprotective effect during reperfusion [51]. Huang and colleagues found that both SIRT1 transfection and treatment with Resv promotes ERK phosphorylation (Thr202/Tyr204) in human fibroblasts [53]. While the mechanism of SIRT1-induced ERK phosphorylation remains to be elucidated, Kobayashi et al. reported that the HDAC inhibitor suppressed MAPK signaling by upregulating Rap1 expression [54], suggesting that SIRT1 may stimulate ERK signaling in a similar way. In our cell model, simulated IR caused a dramatic decrease in the p-ERK/total ERK ratio, which was only reversed by treatment with Resv. To further investigate the molecular pathways underlying the protective effects induced by Resv in IR cardiomyocytes, caspase-3 activity and LDH release were analyzed in the presence of specific MAPK inhibitors. Interestingly, IR cells displayed the highest caspase-3 activity in the presence of ERK inhibitor, an effect that was suppressed by Resv treatment, indicating a prominent role for SIRT1 in protection against apoptotic cell death. SIRT1 overexpression was associated with enhancement of ERK signaling after IR, while incubation with ERK inhibitor decreased the protective effect of SIRT1 overexpression, suggesting that ERK signaling in part underlies SIRT1-mediated protection.

The role that JNK plays in IR is still a matter of debate. A number of *in vitro* and *in vivo* studies have shown that JNK is activated by reoxygenation [55–57]. There is little evidence of JNK activation during the ischemic phase, although some studies suggest it does occur [58]. Whether stress-induced JNK signaling has a protective or pathological effect depends on the cell type, a dichotomy that is apparent in cardiomyocytes. Treatment with JNK-specific inhibitors reduces infarct size and apoptotic cell death following IR [59, 60]. JNK activity also exacerbates the deleterious effects of several proteins involved in IR-induced myocardial injury [60–62]. Moreover, JNK is thought to associate with mitochondria, possibly via interactions with pro-apoptotic proteins [62], while it also regulates nuclear translocation of the mitochondrial apoptosis-inducing factor (AIF) [61, 63]. In other studies performed in cardiac myocytes, inhibition of JNK activity promoted apoptosis and stimulated caspase-3 [64] and

caspase-9 [65] activity in an *in vitro* IR model. It has also been suggested that the cardioprotective effect of JNK may be partly due to Akt activation, a key pro-survival protein in post-ischemic cardiomyocytes [66]. The role of JNK signaling in IR thus remains unclear, possibly due to the complexity of the multistage, interconnected signaling cascades that underlie this process.

In our experimental model, simulated IR triggered an increase in the phospho-JNK/total JNK ratio, with Resv treatment reducing JNK phosphorylation to control levels. Treatment with Trolox or SIRT1 inhibitor, however, did not reduce JNK phosphorylation. Levels of apoptotic cell death were found to be significantly lower in the presence of JNK inhibitor, suggesting a role for these pathways in IR-induced cell death. Cao and coworkers [67] reported that SIRT1 knockdown (using siRNA) in cultured skin keratinocytes stimulates UV-induced JNK activation, an effect that is inhibited by Resv, all of which suggests that SIRT1 precludes JNK activation by UV light. The same group also found that SIRT1 negatively regulates UV-induced JNK activation. This mechanism, which likely proceeds via deacetylation and inhibition of one or several upstream JNK signals, may exist to further protect against UV-induced cell death. Further work is required to determine the mechanism by which SIRT1 negatively regulates JNK activation, however, our findings shed further light on the anti-apoptotic function of SIRT1 activation. Disagreeing results have been obtained by Nasrin and coworkers, who found that JNK1 modifies the function of SIRT1, stimulating its activity and altering its localization [68]. Indeed, our data on the whole suggest an important role for JNK in IR-induced cell death and for SIRT1 in JNK inhibition.

Our findings shed further light on how SIRT1 may regulate cell survival under conditions of oxidative stress. As a cell survival factor, SIRT1 may promote resistance to oxidative stress in mammalian cells. For example, SIRT1 overexpression in normal human IMR-90 fibroblasts reduced H₂O₂-induced apoptosis [69]. Similarly, HEK293T cells treated with serum from calorie-restricted rats displayed increased SIRT1 expression and concomitant inhibition of Bax-mediated apoptosis [70]. Kume et al. [71] showed that SIRT1 overexpression in mesangial cells decreases H₂O₂-induced acetylation of p53. Moreover, neither SIRT1 overexpression nor its knockdown had any effect on H₂O₂-mediated phosphorylation of MAPKs.

The role of p38 during IR is well documented, although reports are conflicting as to its precise effect, with different lines of evidence pointing to protective or deleterious roles for p38. Marked activation of p38 was observed in isolated, perfused rat hearts [72], with several studies showing that p38 activation during ischemia promotes injury [73, 74]. Equally, numerous studies have also demonstrated a protective role for p38 during ischemia [75–77]. In our cell

model, simulated IR triggered an increase in the phospho-p38/total p38 ratio, with Resv treatment reducing p38 phosphorylation to control levels. In the presence of p38 inhibitor, we observed a significant reduction in apoptosis, suggesting a role for these pathways in IR-induced cell death. The exact contribution of p38 kinase to ischemic injury and protection is determined by the isoforms and upstream/downstream pathways involved, as well as the level, duration, mode, and timing of induction. Identifying the beneficial versus deleterious aspects of p38 signaling is a major issue that must be addressed by future studies.

In summary, our data show a cardioprotective role for SIRT1 in IR. During IR, SIRT1 stimulates the expression of cardioprotective molecules while downregulating levels of pro-apoptotic molecules, thereby reducing oxidative stress and inhibiting apoptosis. Our findings also shed further light on the molecular mechanisms by which SIRT1 modulates MAPK signaling via the Akt-ASK1 signaling.

SIRT1 activation may therefore represent a novel approach to protect the heart from ischemic injury.

Acknowledgments This work was supported by Italian MIUR and by Ente Cassa di Risparmio di Firenze.

References

- Murphy E, Steenbergen C (2008) Mechanisms underlying acute protection from cardiac ischemia-reperfusion injury. *Physiol Rev* 88:581–609
- Braunersreuther V, Jaquet V (2012) Reactive oxygen species in myocardial reperfusion injury: from physiopathology to therapeutic approaches. *Curr Pharm Biotechnol* 13:97–114
- Kyriakis JM, Avruch J (2001) Mammalian mitogen-activated protein kinase signal transduction pathways activated by stress and inflammation. *Physiol Rev* 81:807–869
- Alcendor RR, Gao S, Zhai P, Zablocki D, Holle E, Yu X, Tian B, Wagner T, Vatner SF, Sadoshima J (2007) Sirt1 regulates aging and resistance to oxidative stress in the heart. *Circ Res* 100:1512–1521
- Jeong J, Juhn K, Lee H, Kim SH, Min BH, Lee KM, Cho MH, Park GH, Lee KH (2007) SIRT1 promotes DNA repair activity and deacetylation of Ku70. *Exp Mol Med* 39:8–13
- Kaeberlein M, McVey M, Guarente L (1999) The SIR2/3/4 complex and SIR2 alone promote longevity in *Saccharomyces cerevisiae* by two different mechanisms. *Genes Dev* 13:2570–2580
- Motta MC, Divecha N, Lemieux M, Kamel C, Chen D, Gu W, Bultsma Y, McBurney M, Guarente L (2004) Mammalian SIRT1 represses forkhead transcription factors. *Cell* 116:551–563
- Bordone L, Motta MC, Picard F, Robinson A, Jhala US, Apfeld J, McDonagh T, Lemieux M, McBurney M, Szilvasi A, Easlon EJ, Lin SJ, Guarente L (2006) Sirt1 regulates insulin secretion by repressing UCP2 in pancreatic beta cells. *PLoS Biol* 4(2):e31
- Tanno M, Sakamoto J, Miura T, Shimamoto K, Horio Y (2007) Nucleocytoplasmic shuttling of the NAD⁺-dependent histone deacetylase SIRT1. *J Biol Chem* 282:6823–6832
- Ford J, Jiang M, Milner J (2005) Cancer-specific functions of SIRT1 enable human epithelial cancer cell growth and survival. *Cancer Res* 65:10457–10463
- Ohsawa S, Miura M (2006) Caspase-mediated changes in Sir2-alpha during apoptosis. *FEBS Lett* 580:5875–5879
- Alcendor RR, Kirshenbaum LA, Imai S, Vatner SF, Sadoshima J (2004) Silent information regulator 2alpha, a longevity factor and class III histone deacetylase, is an essential endogenous apoptosis inhibitor in cardiac myocytes. *Circ Res* 95:971–980
- Crow MT (2004) Sir-2-like protein: cardioprotection mediated by a longevity gene. *Circ Res* 95:953–956
- Ray PS, Maulik G, Cordis GA, Bertelli AA, Bertelli A, Das DK (1999) The red wine antioxidant resveratrol protects isolated rat hearts from ischemia reperfusion injury. *Free Radic Biol Med* 27:160–169
- Chen CJ, Yu W, Fu YC, Wang X, Li JL, Wang W (2009) Resveratrol protects cardiomyocytes from hypoxia-induced apoptosis through the SIRT1–FoxO1 pathway. *Biochem Biophys Res Commun* 378:389–393
- Namiki A, Brogi E, Kearney M, Kim EA, Wu T, Couffignal T, Varticovski L, Isner JM (1995) Hypoxia induces vascular endothelial growth factor in cultured human endothelial cells. *J Biol Chem* 270:31189–31195
- Bradford MM (1976) A rapid and sensitive method for the quantitation of microgram quantities of protein utilizing the principle of protein-dye binding. *Anal Biochem* 72:248–254
- Drummen GPC, Gadella BM, Post JA, Brouwers JF (2004) Mass spectrometric characterization of the oxidation of the fluorescent lipid peroxidation reporter molecule C11-BODIPY581/591. *Free Rad Biol Med* 36:1635–1644
- Petronilli V, Miotto G, Canton M, Brini M, Colonna R, Bernardi P, Di Lisa F (1999) Transient and long-lasting openings of the mitochondrial permeability transition pore can be monitored directly in intact cells by changes in mitochondrial calcein fluorescence. *Biophys J* 765:725–754
- Fulco M, Cen Y, Zhao P, Hoffman EP, McBurney MW, Sauve AA, Sartorelli V (2008) Glucose restriction inhibits skeletal myoblast differentiation by activating SIRT1 through AMPK-mediated regulation of Nampt. *Dev Cell* 14:661–673
- Fiorillo C, Becatti M, Pensalfini A, Cecchi C, Lanzilao L, Donzelli G, Nassi N, Giannini L, Borchi E, Nassi P (2008) Curcumin protects cardiac cells against ischemia-reperfusion injury: effects on oxidative stress, NF- κ B and JNK pathways. *Free Radic Biol Med* 45:839–846
- Ichijo H, Nishida E, Irie K, ten Dijke P, Saitoh M, Moriguchi T, Takagi M, Matsumoto K, Miyazono K, Gotoh Y (1997) Induction of apoptosis by ASK1, a mammalian MAPKKK that activates SAPK/JNK and p38 signaling pathways. *Science* 275:90–94
- Wang XS, Diener K, Jannuzzi D, Trollinger D, Tan TH, Lichenstein H, Zukowski M, Yao Z (1996) Molecular cloning and characterization of a novel protein kinase with a catalytic domain homologous to mitogen-activated protein kinase kinase. *J Biol Chem* 271:31607–31611
- Kim AH, Khursigara G, Sun X, Franke TF, Chao MV (2001) Akt phosphorylates and negatively regulates apoptosis signal-regulating kinase 1. *Mol Cell Biol* 21:893–901
- Besse S, Bulteau AL, Boucher F, Riou B, Swynghedauw B, de Leiris J (2006) Antioxidant treatment prevents cardiac protein oxidation after ischemia-reperfusion and improves myocardial function and coronary perfusion in senescent hearts. *J Physiol Pharmacol* 57:541–552
- Maddock HL, Mocanu MM, Yellon DM (2002) Adenosine A(3) receptor activation protects the myocardium from reperfusion/reoxygenation injury. *Am J Physiol Heart Circ Physiol* 283: H1307–H1313
- Powers SK, Murlasits Z, Wu M, Kavazis AN (2007) Ischemia-perfusion-induced cardiac injury: a brief review. *Med Sci Sports Exerc* 39:1529–1536

28. Ungvari Z, Labinskyy N, Mukhopadhyay P, Pinto JT, Bagi Z, Ballabh P, Zhang C, Pacher P, Csiszar A (2009) Resveratrol attenuates mitochondrial oxidative stress in coronary arterial endothelial cells. *Am J Physiol Heart Circ Physiol* 297:H1876–H1881
29. Pillai JB, Isbatan A, Imai S, Gupta MP (2005) Poly(ADP-ribose) polymerase-1-dependent cardiac myocyte cell death during heart failure is mediated by NAD⁺ depletion and reduced Sir2alpha deacetylase activity. *J Biol Chem* 280:43121–43130
30. Hsu CP, Zhai P, Yamamoto T, Maejima Y, Matsushima S, Hariharan N, Shao D, Takagi H, Oka S, Sadoshima J (2010) Silent information regulator 1 protects the heart from ischemia/reperfusion. *Circulation* 123:2170–2182
31. Pacholec M, Bleasdale JE, Chrnyk B, Cunningham D, Flynn D, Garofalo RS, Griffith D, Griffor M, Loulakis P, Pabst B, Qiu X, Stockman B, Thanabal V, Varghese A, Ward J, Withka J, Ahn K (2010) SRT1720, SRT2183, SRT1460, and resveratrol are not direct activators of SIRT1. *J Biol Chem* 285:8340–8351
32. Das S, Khan N, Mukherjee S, Bagchi D, Gurusamy N, Swartz H, Das DK (2008) Redox regulation of resveratrol-mediated switching of death signal into survival signal. *Free Radic Biol Med* 44:82–90
33. Michan S, Sinclair D (2007) Sirtuins in mammals: insights into their biological function. *Biochem J* 405:1–13
34. Brunet A, Sweeney LB, Sturgill JF, Chua KF, Greer PL, Lin Y, Tran H, Ross SE, Mostoslavsky R, Cohen HY, Hu LS, Cheng HL, Jedrychowski MP, Gygi SP, Sinclair DA, Alt FW, Greenberg ME (2004) Stress-dependent regulation of FOXO transcription factors by the SIRT1 deacetylase. *Science* 303:2011–2015
35. Oudit GY, Sun H, Kerfant BG, Crackower MA, Penninger JM, Backx PH (2004) The role of phosphoinositide-3 kinase and PTEN in cardiovascular physiology and disease. *J Mol Cell Cardiol* 37:449–471
36. Matsui T, Li L, del Monte F, Fukui Y, Franke T, Hajjar R, Rosenzweig A (1999) Adenoviral gene transfer of activated PI 3-kinase and Akt inhibits apoptosis of hypoxic cardiomyocytes in vitro. *Circulation* 100:2373–2379
37. Matsui T, Tao J, del Monte F, Lee KH, Li L, Picard M, Force TL, Franke TF, Hajjar RJ, Rosenzweig A (2001) Akt activation preserves cardiac function and prevents injury after transient cardiac ischemia in vivo. *Circulation* 104:330–335
38. Bhuiyan MS, Shibuya M, Shioda N, Moriguchi S, Kasahara J, Iwabuchi Y, Fukunaga K (2007) Cytoprotective effect of bis(1-oxy-2-pyridinethiolato)oxovanadium (IV) on myocardial ischemia/reperfusion injury elicits inhibition of Fas ligand and Bim expression and elevation of FLIP expression. *Eur J Pharmacol* 571:180–188
39. Bhuiyan MS, Shioda N, Fukunaga K (2008) Targeting protein kinase B/Akt signaling with vanadium compounds for cardioprotection. *Expert Opin Ther Targets* 12:1217–1227
40. Takada Y, Hashimoto M, Kasahara J, Aihara K, Fukunaga K (2004) Cytoprotective effect of sodium orthovanadate on ischemia/reperfusion-induced injury in the rat heart involves Akt activation and inhibition of fodrin breakdown and apoptosis. *J Pharmacol Exp Ther* 311:1249–1255
41. Yano S, Morioka M, Fukunaga K, Kawano T, Hara T, Kai Y, Hamada J, Miyamoto E, Ushio Y (2001) Activation of Akt/Protein Kinase B contributes to induction of ischemic tolerance in the CA1 subfield of gerbil hippocampus. *J Cereb Blood Flow Metab* 21:351–360
42. Zhang R, Luo D, Miao R, Bai L, Ge Q, Sessa WC, Min W (2005) Hsp90-Akt phosphorylates ASK1 and inhibits ASK1-mediated apoptosis. *Oncogene* 24:3954–3963
43. Choudhary C, Kumar C, Gnad F, Nielsen ML, Rehman M, Walther TC, Olsen JV, Mann M (2009) Lysine acetylation targets protein complexes and co-regulates major cellular functions. *Science* 325:834–840
44. Finkel T, Deng CX, Mostoslavsky R (2009) Recent progress in the biology and physiology of sirtuins. *Nature* 460:587–591
45. Milne JC, Lambert PD, Schenk S, Carney DP, Smith JJ, Gagne DJ, Jin L, Boss O, Perni RB, Vu CB, Bemis JE, Xie R, Disch JS, Ng PY, Nunes JJ, Lynch AV, Yang H, Galonek H, Israelian K, Choy W, Iffland A, Lavu S, Medvedik O, Sinclair DA, Olefsky JM, Jirousek MR, Elliott PJ, Westphal CH (2007) Small molecule activators of SIRT1 as therapeutics for the treatment of type 2 diabetes. *Nature* 450:712–716
46. Sundaresan NR, Pillai VB, Wolfgeher D, Samant S, Vasudevan P, Parekh V, Raghuraman H, Cunningham JM, Gupta M, Gupta MP (2011) The deacetylase SIRT1 promotes membrane localization and activation of Akt and PDK1 during tumorigenesis and cardiac hypertrophy. *Sci Signal* 19(4):ra46
47. Chang HY, Nishitoh H, Yang X, Ichijo H, Baltimore D (1998) Activation of apoptosis signal-regulating kinase 1 (ASK1) by the adapter protein Daxx. *Science* 281:1860–1863
48. Chen Z, Seimiya H, Naito M, Mashima T, Kizaki A, Dan S, Imaizumi M, Ichijo H, Miyazono K, Tsuruo T (1999) ASK1 mediates apoptotic cell death induced by genotoxic stress. *Oncogene* 18:173–180
49. Tobiume K, Saitoh M, Ichijo H (2002) Activation of apoptosis signal-regulating kinase 1 by the stress-induced activating phosphorylation of pre-formed oligomer. *J Cell Physiol* 191:95–104
50. Yue TL, Wang C, Gu JL, Ma XL, Kumar S, Lee JC, Feuerstein GZ, Thomas H, Maleeff B, Ohlstein EH (2000) Inhibition of extracellular signal-regulated kinase enhances ischemia/reoxygenation-induced apoptosis in cultured cardiac myocytes and exaggerates reperfusion injury in isolated perfused heart. *Circ Res* 86:692–699
51. Hausenloy DJ, Tsang A, Yellon DM (2005) The reperfusion injury salvage kinase pathway: a common target for both ischemic preconditioning and postconditioning. *Trends Cardiovasc Med* 15:69–75
52. Thomas CJ, Ng DC, Patsikatheodorou N, Limengka Y, Lee MW, Darby IA, Woodman OL, May CN (2011) Cardioprotection from ischaemia-reperfusion injury by a novel flavonol that reduces activation of p38 MAPK. *Eur J Pharmacol* 658:160–167
53. Huang J, Gan Q, Han L, Li J, Zhang H, Sun Y, Zhang Z, Tong T (2008) SIRT1 overexpression antagonizes cellular senescence with activated ERK/S6k1 signaling in human diploid fibroblasts. *PLoS One* 3:e1710
54. Kobayashi Y, Ohtsuki M, Murakami T, Kobayashi T, Sutheesophon K, Kitayama H, Kano Y, Kusano E, Nakagawa H, Furukawa Y (2006) Histone deacetylase inhibitor FK228 suppresses the Ras-MAP kinase signaling pathway by upregulating Rap1 and induces apoptosis in malignant melanoma. *Oncogene* 25:512–524
55. Fryer RM, Patel HH, Hsu AK, Gross GJ (2001) Stress-activated protein kinase phosphorylation during cardioprotection in the ischemic myocardium. *Am J Physiol Heart Circ Physiol* 281:H1184–H1192
56. Laderoute KR, Webster KA (1997) Hypoxia/reoxygenation stimulates jun kinase activity through redox signaling in cardiac myocytes. *Circ Res* 80:336–344
57. Yin T, Sandhu G, Wolfgang CD, Burrier A, Webb RL, Rigel DF, Hai T, Whelan J (1997) Tissue specific pattern of stress kinase activation in ischemic/reperfused heart and kidney. *J Biol Chem* 272:19943–19950
58. Ping P, Zhang J, Huang S, Cao X, Tang XL, Li RCX, Zheng YT, Qiu Y, Clerk A, Sugden P, Han J, Bolli R (1999) PKC-dependent activation of p46/p54 JNKs during ischemic preconditioning in conscious rabbits. *Am J Physiol Heart Circ Physiol* 277:H1771–H1785
59. Ferrandi C, Ballerio R, Gaillard P, Carboni S, Vitte P, Gotteland J, Cirillo R (2004) Inhibition of c-Jun N-terminal kinase

- decreases cardiomyocyte apoptosis and infarct size after myocardial ischemia and reperfusion in anaesthetized rats. *Br J Pharmacol* 142:953–960
60. Milano G, Morel S, Bonny C, Samaja M, von Segesser LK, Nicod P, Vassalli G (2007) A peptide inhibitor of c-Jun NH2-terminal kinase reduces myocardial ischemia-reperfusion injury and infarct size in vivo. *Am J Physiol Heart Circ Physiol* 292:H1828–H1835
 61. Aleshin A, Ananthakrishnan R, Li Q, Rosario R, Lu Y, Qu W, Song F, Bakr S, Szabolcs M, D'Agati V, Liu R, Homma S, Schmidt AM, Yan SF, Ramasamy R (2008) RAGE modulates myocardial injury consequent to LAD infarction via impact on JNK and STAT signaling in a murine model. *Am J Physiol Heart Circ Physiol* 294:H1823–H1832
 62. Remondino A, Kwon SH, Communal C, Pimentel DR, Sawyer DB, Singh K, Colucci WS (2003) β -Adrenergic receptor-stimulated apoptosis in cardiac myocytes is mediated by reactive oxygen species/c-Jun NH2-terminal kinase-dependent activation of the mitochondrial pathway. *Circ Res* 92:136–138
 63. Zhang DW, Shao J, Lin J, Zhang N, Lu BJ, Lin SC, Dong MQ, Han J (2009) RIP3, an energy metabolism regulator that switches TNF-induced cell death from apoptosis to necrosis. *Science* 325:332–336
 64. Engelbrecht AM, Niesler C, Page C, Lochner A (2004) p38 and JNK have distinct regulatory functions on the development of apoptosis during simulated ischaemia and reperfusion in neonatal cardiomyocytes. *Basic Res Cardiol* 99:338–350
 65. Dougherty CJ, Kubasiak LA, Prentice H, Andreka P, Bishopric NH, Webster KA (2002) Activation of c-Jun N-terminal kinase promotes survival of cardiac myocytes after oxidative stress. *Biochem J* 362:561–571
 66. Shao Z, Bhattacharya K, Hsieh E, Park L, Walters B, Germann U, Wang YM, Kyriakis J, Mohanlal R, Kuida K, Namchuk M, Salituro F, Yao YM, Hou WM, Chen X, Aronovitz M, Tsichlis PN, Bhattacharya S, Force T, Kilter H (2006) c-Jun N-terminal kinases mediate reactivation of Akt and cardiomyocyte survival after hypoxic injury in vitro and in vivo. *Circ Res* 98:111–118
 67. Cao C, Lu S, Kivlin R, Wallin B, Card E, Bagdasarian A, Tamakloe T, Wang WJ, Song X, Chu WM, Kouttab N, Xu A, Wan Y (2009) SIRT1 confers protection against UVB- and H₂O₂-induced cell death via modulation of p53 and JNK in cultured skin keratinocytes. *J Cell Mol Med* 13:3632–3643
 68. Nasrin N, Kaushik VK, Fortier E, Wall D, Pearson KJ, de Cabo R, Bordone L (2009) JNK1 phosphorylates SIRT1 and promotes its enzymatic activity. *PLoS One* 4:e8414
 69. Luo J, Nikolaev AY, Imai S, Chen D, Su F, Shiloh A, Guarente L, Gu W (2001) Negative control of p53 by Sir2alpha promotes cell survival under stress. *Cell* 107:137–148
 70. Cohen HY, Miller C, Bitterman KJ, Wall NR, Hekking B, Kessler B, Howitz KT, Gorospe M, de Cabo R, Sinclair DA (2004) Calorie restriction promotes mammalian cell survival by inducing the SIRT1 deacetylase. *Science* 305:390–392
 71. Kume S, Haneda M, Kanasaki K, Sugimoto T, Araki S, Isono M, Isshiki K, Uzu T, Kashiwagi A, Koya D (2006) Silent information regulator 2 (SIRT1) attenuates oxidative stress-induced mesangial cell apoptosis via p53 deacetylation. *Free Rad Biol Med* 40:2175–2182
 72. Bogoyevitch MA, Gullepie-Brown J, Ketterman A, Fuller S, Ben-Levy R, Ashworth A, Marshall CJ, Sugden P (1996) Stimulation of the stress-activated mitogen-activated protein kinase subfamilies in perfused heart: p38/RK mitogen-activated protein kinases and c-Jun N-terminal kinases are activated by ischemia/reperfusion. *Circ Res* 79:162–173
 73. Bell JR, Eaton P, Shattock MJ (2008) Role of p38-mitogen-activated protein kinase in ischaemic preconditioning in rat heart. *Clin Exp Pharmacol Physiol* 35:126–134
 74. Sanada S, Kitakaze M, Papst P, Hatanaka K, Asanuma H, Aki T, Shinozaki Y, Ogita H, Node K, Takashima S, Asakura M, Yamada T, Fukushima T, Ogai A, Kuzuya T, Mori H, Terada N, Yoshida K, Hori M (2001) Role of phasic dynamism of p38 mitogenactivated protein kinase activation in ischemic preconditioning of the canine heart. *Circ Res* 88:175–180
 75. Martin J, Hickey E, Weber L, Dillmann WH, Mestrlil R (1999) Influence of phosphorylation and oligomerization on the protective role of the small heat shock protein 27 in rat adult cardiomyocytes. *Gene Exp* 7:349–355
 76. Mocanu MM, Baxter GF, Yue Y, Critz SD, Yellon DM (2000) The p38 MAPK inhibitor, SB203580, abrogates ischaemic preconditioning in rat heart but timing of administration is critical. *Basic Res Cardiol* 95:472–478
 77. Maulik N, Yoshida T, Zu YL, Sato M, Banerjee A, Das DK (1998) Ischemic preconditioning triggers tyrosine kinase signaling: a potential role for MAPKAP kinase 2. *Am J Physiol Heart Circ Physiol* 275:H1857–H1864